Lanthanide impurity level location in GaN, AlN, and ZnO

P. Dorenbos*, E. van der Kolk
Faculty of Applied Sciences, Delft University of Technology, Mekelweg 15, 2629JB Delft, Netherlands

ABSTRACT

A method that has proven succesful in locating the energy levels of divalent and trivalent lanthanide ions (Ce, Pr,..., Eu,...Yb, Lu) in wide band gap inorganic compounds like YPO_4 and CaF_2 is applied to locate lanthanide levels in the wideband semiconductors GaN, AlN, their solid solutions $Al_xGa_{1-x}N$, and ZnO. The proposed schemes provide a description of relevant optical and luminescence properties of these lanthanide doped semiconductors. Especially, the relation between thermal quenching of Tb^{3+} emission and the location of the energy levels is explained.

Keywords: GaN, AlN, ZnO, lanthanides, localized states

1. INTRODUCTION

There is strong interest in the electronic and optical properties of lanthanide doped III-V semiconductors like GaN, AlN and their alloys $Al_xGa_{1-x}N$ ($0 \leq x \leq 1$). Recently the II-VI compound ZnO is also subject of extensive research. Because of the wide band gap, as compared to e.g. InN or GaP, these compounds are optically transparent [1,2], and many studies were performed on the luminescence of lanthanide impurities like Pr^{3+}, Nd^{3+}, Sm^{3+}, Eu^{3+}, Tb^{3+}, Dy^{3+}, Er^{3+}, Tm^{3+}, and Yb^{3+}. Divalent lanthanides are not stable in these types of compounds. In the case of GaN doped with Tm^{3+}, Er^{3+}, and Eu^{3+} blue, green, and red luminescence was demonstrated [3,4,5]. Unfortunately, $GaN:Ln^{3+}$ is still not applied as thin-film electroluminescent material because of the low luminescence efficiency at room temperature [6,7]. It is therefore of interest to understand the causes for luminescence quenching.

By alloying GaN with AlN the room temperature luminescence efficiency of Eu^{3+} and Tb^{3+} increases with increasing Al content [8]. The factors that determine luminescence efficiency of lanthanide ions in $Al_xGa_{1-x}N$ are still not understood. Often the lanthanide ions are treated as iso-electronic impurities [9]. Since lanthanide ions have different size and electro-negativity compared to the cation they substitute for (Ga^{3+} or Al^{3+}), they create a short range potential that may trap a free charge carrier. Subsequently the counter charge carrier is trapped forming an exciton bound near or at the lanthanide ion. The energy of the bound exciton can be transferred to excite the 4f core of the lanthanide ion which eventually leads to the luminescence. In this model the thermal quenching of emission is attributed to energy back transfer from the excited 4f-core to the bound exciton configuration followed by non-radiative recombination [9]. From the Arrhenius type behavior of luminescence intensity and luminescence decay time, the activation energy for energy back transfer has been determined for Eu^{3+} and Tb^{3+} in various compositions of $Al_xGa_{1-x}N$ [8,10,11].

The fact that the 4f-shell of a trivalent lanthanide ion may accept or donate an electron from or to the energy bands of a III-V compound with $Ln^{3+} \rightarrow Ln^{2+}$ or $Ln^{3+} \rightarrow Ln^{4+}$ valence change is not considered in the current models on luminescence excitation and quenching. Such valence changes are well known in wide band gap oxide and fluoride compounds and are likely to be important in the III-V semiconductors as well. Two basic questions need to be answered to understand energy transfer and charge trapping phenomena: 1) What is the location of the lanthanide (Ln) ion energy levels relative to the conduction band (CB) and valence band (VB) of the hosting compound, and 2) how do lanthanide energy level locations affect room temperature luminescence efficiency, thermal quenching, charge carrier trapping, and charge carrier donating processes?

These questions were asked long time ago in the field of lanthanide doped wide band gap (6-10 eV) compounds applied as lighting, storage, or display phosphors. Recently methods became available that predict level locations for all the lanthanides in inorganic compounds [12,13,14]. Recently we applied those methods for the first time to GaN, AlN, and

---

* p.dorenbos@tudelft.nl

Gallium Nitride Materials and Devices II, edited by Hadis Morkoc, Cole W. Litton,
Proc. of SPIE Vol. 6473, 647313, (2007) · 0277-786X/07/$18 · doi: 10.1117/12.698977

their alloys $Al_xGa_{1-x}N$ and proposed level schemes with the location of the ground states of all divalent and all trivalent lanthanides [15,16] relative to the valence and conduction band of those compounds. The schemes reveal which lanthanide ions are potential electron traps and which are potential hole traps. It also reveals mechanisms for luminescence quenching of, for example, the red $^5D_0$- $^7F_2$ Eu^{3+} emission or the $^5D_4$- ^7F_J Tb^{3+} emissions, or the presence or absence of $^5D_3$- ^7F_J Tb^{3+} emission.

Because this method is still relatively new and not yet adopted in the field of lanthanide doped III-V and II-VI semiconductor research, we will review the method in this work and illustrate how the schemes for GaN and AlN and their alloys were made. Also the main difference with schemes in wide band gap inorganic compounds like YPO_4 is illustrated. For the first time a scheme for the lanthanide ions in ZnO is presented. This paper is organized as follows. First the historic developments leading to the method of level positioning is briefly presented. Then it is applied to place the level energies of the divalent and trivalent lanthanide ions in GaN [15] and AlN. Next we demonstrate how the luminescence properties of Tb^{3+} emission changes with the alloying parameter x in $Al_xGa_{1-x}N$, and finally a tentative scheme for ZnO is presented. It will be shown that energy levels of lanthanides in compounds behave in a rather systematic manner with changing type of lanthanide ion, changing valence of the lanthanide ion and change of hosting compound.

2. METHOD OF LANTHANIDE LEVEL LOCATION

The luminescence properties of divalent and trivalent lanthanide doped inorganic compounds have been subject of extensive research since the sixtees of the previous century. Research on luminescence phosphors for tube lighting (TL) eventually lead to the development of the widely applied three color TL phosphor lamp. Lanthanide doped phosphors also found their way in display screens for television and computers, and nowadays lanthanide doped phosphors are being developed for the new generation of light emitting diode (LED) based lighting systems. In all that research a wealth of data and knowledge was generated on the energy levels of the lanthanide ions, and how they are affected by the host compound. The numerous levels of the $4f^n$ configuration are conveniently represented by the so-called Dieke diagram. Transitions between 4f states lead to narrow line emission of high color purity and wavelength that is almost entirely determined by the atomic properties of the lanthanide ion and hardly influenced by the crystalline environment. The red emission from the $^5D_0 \rightarrow {}^7F_2$ transition in Eu^{3+} or the green emission from the $^5D_4 \rightarrow {}^7F_5$ transition in Tb^{3+} are very important for luminescence applications. The situation is different for the levels of the higher energy 5d configuration. The orbitals of these levels extent to the perifery of the lanthanide ion and consequently have a strong interaction with neighboring ligands. The energy of interconfigurational transitions between levels of the 4f configration and the 5d configuration then depend strongly on crystalline environment and therewith on the choice of host material and the site occupied by the lanthanide. For example the wavelength of the dipole allowed and fast 5d-4f emission in Ce^{3+} may vary from as short as 250 nm in fluoride compounds to 600 nm in sulfide compounds [17].

The theory of 4f levels was already developed in the sixtees and seventies of the 20th century. Knowledge on how the energy of the 5d states changes with type of compound and type of lanthanide was until recently much less developed. By collecting data from the literature on 5d-4f transitions of all thirteen lanthanide ions (both trivalent and divalent) in numerous different types of compounds, a penomenological model was developed by Dorenbos [18]. It was shown that the energy lowering of the 5d state of a lanthanide ion in a compound as compared to the value for the free lanthanide ion is in first approximation independent on the type of lanthanide ion. This allows the definition of a single parameter, the so-called redshift $D(3+,A)$, that gives the energy lowering of the 5d state of all the trivalent lanthanides in a specific compound A. Values for $D(3+,A)$ and also $D(2+,A)$ are now available for more than 500 different compounds [17,19]. The introduction of the redshift parameter has proven very succesful in predicting the energy of 4f-5d transitions of lanthanide ions in compounds and has developed into a useful tool for analyzing excitation and absorption spectra.

Parallel to the development of the phenomenological model on 4f-5d transition energy, the theory of 5d energy levels has been developed. Some theories relate to models that describe the 5d states as function of type of lanthanide ion [20,21]. These theories still require experimental information on the 5d energies for Ce^{3+} in a compound as input. Fully *ab initio* theoretical models and calculations on Ce^{3+} 4f-5d transitions in compounds are also appearing [22,23].

All the above studies and theories relate to energy differences; not to the absolute energy of lanthanide levels relative to for example the conduction band bottom or the valence band top of the hosting compound. Absolute level location has always been subject of speculation past decades and was regarded as an unsolvable problem. However, locating the energy levels appears actually relative easy. There are two approaches; one is by measuring the locations by a variety of experimental techniques, the other is again by developing phenomenological models combined with available experimental data. X-ray or ultraviolet photoelectron spectroscopy (XPS or UPS) can be used to determine the binding energy of 4f electrons relative to the binding energy of valence band electrons. Thiel *et al.* [14] performed a study to determine the 4f ground state energies of the *trivalent* lanthanide ions in a compound, i.e. $Y_3Al_5O_{12}$, with UPS techniques. A method to determine the level location of *divalent* lanthanide ions is by means of charge transfer spectroscopy. When an electron is excited from the valence band, i.e., from a neigboring anion ligand, to a trivalent lanthanide ion the final state of the corresponding divalent lanthanide ion is obtained. The energy of the transition then provides a measure for the location of the divalent ground state above the valence band. Other methods make use of photoconductivity where electrons are excited from the lanthanide ground state to the conduction band thus providing information on the ground state energy relative to the conduction band bottom.

All these experimental methods were applied to determine level locations of lanthanide ions in compounds. However, the methods were often limited to one compound and one lanthanide ion, and did not provide an overview to derive a succesful predicting model that could be applied to all lanthanides in different compounds. Thiel *et a*l. [14] were the first to propose a model based on their UPS results. They combined their findings with the model of Dorenbos on 4f-5d differences to develop a general model to locate both 4f and 5d states of the trivalent lanthanides in a compounds once the level positions of only one of the lanthanide ions was established. Nakazawa proposed a model that predicts the energy of charge transfer to all trivalent lanthanide ions once that of only one of them is known [24]. Dorenbos used a related approach and combined it with his model on 4f-5d energy difference to obtain a model that predicts all the 4f and 5d ground state levels of the divalent lanthanides in compound with only three parameters, i.e., the redshift $D(2+,A)$, the energy $E^{CT}(3+,Eu)$ of charge transfer to Eu^{3+}, and the bandgap E_{VC} of the hosting compound [12]. Values for these three parameters for many different compouns were collected [13]. By analogy, the same method could be applied for the trivalent lanthanide ions. It requires the energy of charge transfer to a tetravalent lanthanide ion. However, those values are not available abundantly because in most compounds the tetravalent charge state is not stable. In stead one should attempt to determine experimentally one level of one lanthanide as a sort of anchor point. The model then predict the location of the levels of the other lanthanides. The absolute location of the lowest 5d state of Ce^{3+} relative to the conduction band bottom may play such a role.

The above method to locate the lanthanide energy levels was applied by us already to the wide band gap compounds CaF_2 and YPO_4 [12] and the smaller band gap compounds $CaGa_2S_4$ [25] and $LaBr_3$ [26]. $LnC_{25}H_{38}N_4S_6$ with the soft donor ligands from nitrogen and sulphur is the first organic compound where the method was applied by Liu *et al*. [27].

Lanthanide doped YPO_4 has been a model compound for various studies. Van Pieterson *et al.* [20,21] determined accurately the energy of the states of the 5d configuration of most of the trivalent lanthanide ions. The energies of the 4f-5d transition are in good agreement with the Dorenbos model. Nakazawa [24] determined the energy of CT to trivalent lanthande ions in YPO_4. Figure 1 shows the level scheme for the wide band gap compound YPO_4. The bottom of the conduction band (mobility band gap) is placed slightly above the exciton creation energy E^{ex}. In the scheme the lanthanide energy levels are placed as function of the number of electrons n in the 4f shell of the trivalent lanthanide ion. Starting on the left side with La^{2+} (n=1) and Ce^{3+} (n=1) and ending on the right side with Yb^{2+} and Lu^{3+} with n=14. The observed O^{2-} to Ln^{3+} CT transition energies are shown as upward pointing arrows in Fig. 1. By connecting the endpoints we observe the famous double seated curve that reflects the variation in binding energy of the 4f electron in the free lanthanide ions. This is a universal curve determined by the intrinsic property of the lanthanide ion. It reappears in all compounds. Almost the same universal curve applies for the trivalent lanthanide ions. We only need to know the ground state location of Ce^{3+} and then the universal curve provides the location of the other lanthanides.

The scheme for the lanthanides in YPO_4 shows that the ground state energies are lowest, or the binding energies are largest, for the lanthanide ions with half (Gd^{3+}, Eu^{2+}) and completely filled (Lu^{3+}, Yb^{2+}) 4f orbitals, and highest for the ones with one (Ce^{3+}, La^{2+}) and eight (Tb^{3+}, Gd^{2+}) electrons. The scheme also shows that the energy of the lowest 5d state of the trivalent lanthanides is relatively constant through the lanthanide series, i.e. with n.

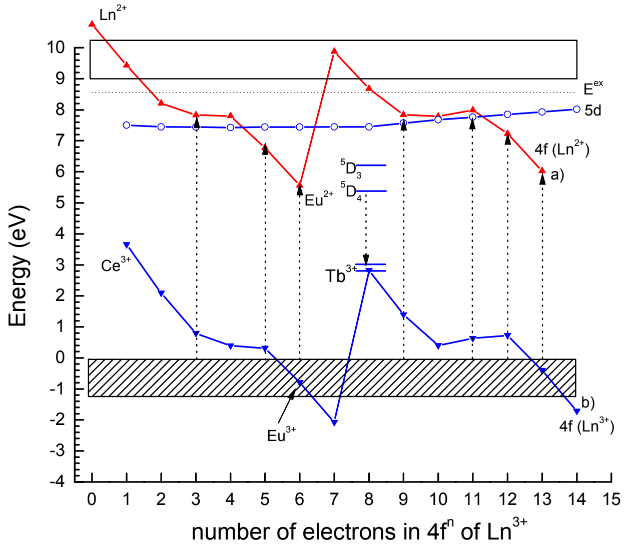

Fig. 1 The lanthanide energy level scheme in YPO_4. Up pointing arrows indicate observed energies for charge transfer from the top of the valence band to the trivalent lanthanide ions. The double seated shape of curve a) connects the ground state energies of the divalent lanthanides. The double seated curve b) connects the ground state energies of the trivalent lanthanides. ΔE(Eu)=6.35 eV is the energy between the ground state of Eu^{2+} and Eu^{3+}.

During the past couple of years several schemes like in Fig. 1 were constructed. It appears that the parameters to place the levels for the divalent lanthanide ions are not entirely independent from those to place the trivalent ones. For example D(3+,*A*) is approximately linearly related with D(2+,*A*) and also the energy difference between the ground 4f state of Eu^{2+} with the ground 4f state of Eu^{3+} appears relatively constant. This difference denoted as ΔE(Eu) amounts about 6.4 eV for YPO_4. This value tends to decrease slightly with smaller value for the band gap of the hosting compound and for $CaGa_2S_4$ a difference of 5.7 eV was found [25].

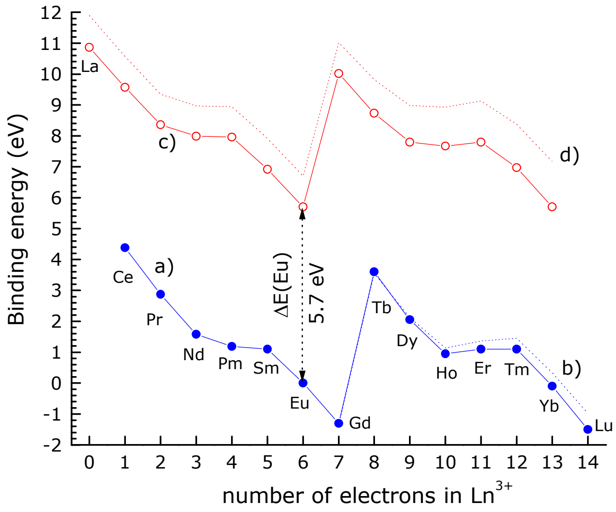

Fig. 2 Universal behavior of 4f-electron binding energies of (a) trivalent and (c) divalent lanthanide ions in sulfide, iodide, and nitride compounds with ΔE(Eu)≈5.7±0.3 eV. Curves b) and c) pertain to fluoride and oxide compounds with ΔE(Eu)≈6.7±0.3 eV.

Our knowledge on lanthanide level location in compounds is conveniently gathered in Fig. 2. Curves a) and c) connect the $4f^n$ ground state binding energies of the trivalent lanthanide and divalent lanthanide ions, respectively, where the zero of energy is chosen at the Eu^{3+} ground state. Although the double seated shape is universal there appears a slight variation of the shape with type of compound. In wide band gap fluorides and oxides like YPO_4 in Fig. 1, the slightly tilted curves b) and d) are appropriate where the binding energy for large *n* is slightly reduced 0.5 eV as compared to bromide or sulfide compounds [13,25].

The energy difference ΔE(Eu) between the $4f^6$ ground state of Eu^{3+} and the $4f^7$ ground state of Eu^{2+} can be used to express the dependence of binding energy on the lanthanide charge. ΔE(Eu) appears to scale with the type of anions in the compound. It decreases from ≈6.35 eV, see curve d), for the oxide compound YPO_4 to ≈5.7 eV, see curve c) for the sulfide compound $CaGa_2S_4$ [25,26] and the bromide compound $LaBr_3$ [26]. For GaN, AlN, and their alloys curves a) and c) to represent the change in binding energy with type of lanthanide ion or *n* will be used. For ZnO we will like for YPO_4 use curves b) and d).

3. LEVEL SCHEMES OF GAN, ALN, AND ZNO

To construct the energy level schemes we only need to use the appropriate curves in Fig. 2 and place them at the proper position relative to the valence band and the conduction band of the host compound. We expect that in the nitride compounds GaN, AlN, and their alloys the value for ΔE(Eu) should be around 5.7 ± 0.3 eV. For ZnO a value of 6.4 ± 0.3 eV typical for oxide compounds is expected. The bandgap of the compounds is well known. Information from luminescence excitation or optical absorption will be used to determine the energy of the CT band and to place the divalent lanthanide levels. We will use information on luminescence quenching of Tb^{3+} to locate the trivalent lanthanides.

3.1 GaN

In [16] we presented the level scheme for GaN which is, in slightly modified form, reproduced in Fig. 3. The band gap of GaN is 3.42 eV which defines the difference between the top of the valence band and the bottom of the conduction band as shown in Fig. 3. To locate the divalent lanthanide ground states by means of curve c) in Fig. 2 we need information on the energy of charge transfer to Eu^{3+}. We used a value of 3.15 eV as derived from [28,6].

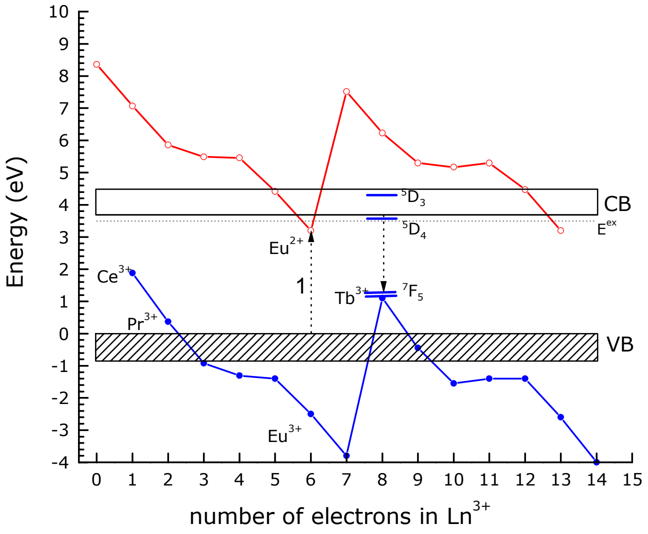

Fig. 3 The proposed lanthanide level locations in GaN. The top of the valence band is at energy zero. Arrow 1 indicates the charge transfer transition from nitrogen to Eu^{3+}. The location of relevant energy levels of Tb^{3+} are indicated.

To place the energy levels of the trivalent lanthanides, we made use of a different approach. The green $^5D_4 \rightarrow {}^7F_5$ emission line of Tb^{3+} is quenched at low temperature in GaN. The quenching was attributed to energy back transfer from Tb^{3+} to the host lattice. We have a different explanation [15,16]. The quenching, in our opinion, is caused by thermally excited ionization of the $^5D_4$ electron to the conduction band of GaN. The reported 8 meV quenching energy barrier for the green emission from the $^5D_4$ level [11] of Tb^{3+} should then be interpreted as the energy difference between the $^5D_4$ state and the conduction band bottom. This locates the $^5D_4$ state and therewith also the ground state energy of Tb^{3+}. With curve a) of Fig. 2 then all ground state energy levels for the trivalent lanthanides are obtained. The resulting level scheme of Fig. 3 has $\Delta E(Eu)$ =5.85 eV. Note that in the scheme of Fig. 3 the higher energy $^5D_3$ level of Tb^{3+} is inside the conduction band. An electron excited to $^5D_3$ immediately auto-ionizes to conduction band states. This explains the absence [11] of $^5D_3$ - ^7F_J Tb^{3+} emission in GaN even at He temperature.

3.2 AlN and $Al_xGa_{1-x}N$

The method to determine the level location in AlN is the same as for GaN. In the work of Lozykowski *et al.* [29] the luminescence emission and its excitation spectra are presented for Eu^{3+}. The excitation spectrum of Eu^{3+} emission reveals a very clear 0.5 eV wide (FWHM) excitation band at 355 nm. We again attribute this band to the charge transfer (CT) to Eu^{3+} and it places the ground state of Eu^{2+}. Note that the scheme predicts the energy of charge transfer to Yb^{3+} at 3.49 eV (355 nm). An experimental observation of that band would strongly support the proposed level locations.

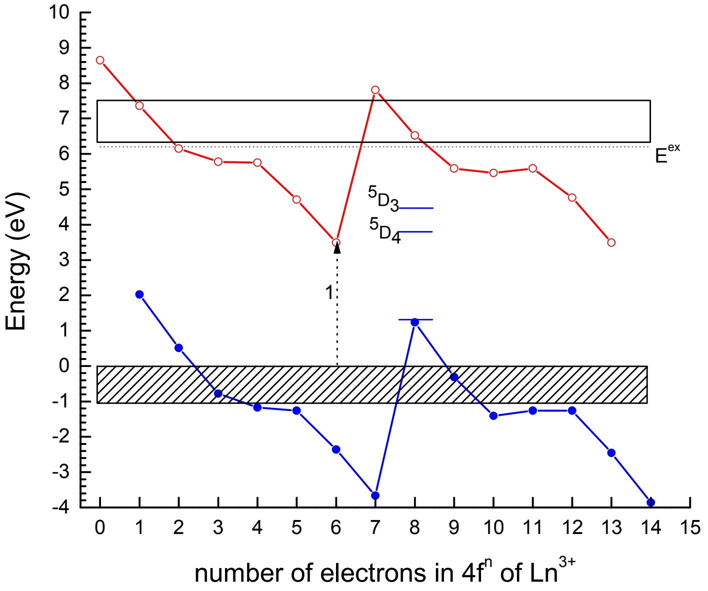

Fig. 4 The proposed location of the lowest 4f states of divalent and trivalent lanthanides in AlN. The top of the valence band is at energy zero. The AlN exciton state is at 6.2 eV. Optical transitions (arrows) and relevant excited and ground state 4f level of Tb^{3+} (bars) are shown.

By assuming that $\Delta E(Eu)$ = 5.85 eV, i.e., the same value as found for GaN, the levels of the trivalent lanthanide ions can be placed. We are aware that at this stage the assumption on the value for $\Delta E(Eu)$ and the assignment of the 355 nm band to the CT of Eu^{3+} may seem tentative. However, based on the electronegativity of the nitride anion we do expect the energy of the CT band to Eu^{3+} around 3.0 to 3.5 eV [15,16,13]. We also expect that the energy of the CT band to Eu^{3+} on the Al site in AlN is at higher energy than when on the Ga site in GaN. The smaller size of Al creates a larger negative Madelung potential at the Al site which raises the energy of electron levels relative to the valence band [13]. We can obtain more supporting evidence by using information available on Tb^{3+} emission. The $^5D_3$ and $^5D_4$ levels of Tb^{3+} are placed in the diagram of Fig. 4. The diagram does explain the presence of Tb^{3+} $^5D_3$-^7F_J emissions. Contrary to GaN, the $^5D_3$ state is well below the conduction band and $^5D_3$ emission is observed in AlN.

Alloying GaN with AlN forming $Al_xGa_{1-x}N$ has various interesting consequences. Al^{3+} is smaller than Ga^{3+} and the lattice parameter decreases from 446 pm for GaN to 435 pm for AlN [30]. At the same time the band gap increases with x according to

$$E_g(x) = 3.42(1-x) + 6.2x - 0.98x(1-x) \qquad (1)$$

where 3.42 eV, 6.2 eV, and 0.98 eV represent the band gap of GaN, AlN and the so-called bowing parameter, respectively [1,2,31].

Using Eq. (1) one may construct the level scheme of a lanthanide ion in $Al_xGa_{1-x}N$ alloys as function of the composition parameter x. In Fig. 5 this is illustrated for the Tb^{3+} levels. The energy of the conduction band bottom is given by Eq. (1). For x=0 and x=1 the locations of the Tb^{3+} 4f states are taken from the schemes of GaN and AlN In Fig. 3 and Fig. 4. Straight lines connecting those 4f states provide the level locations for all other x values.

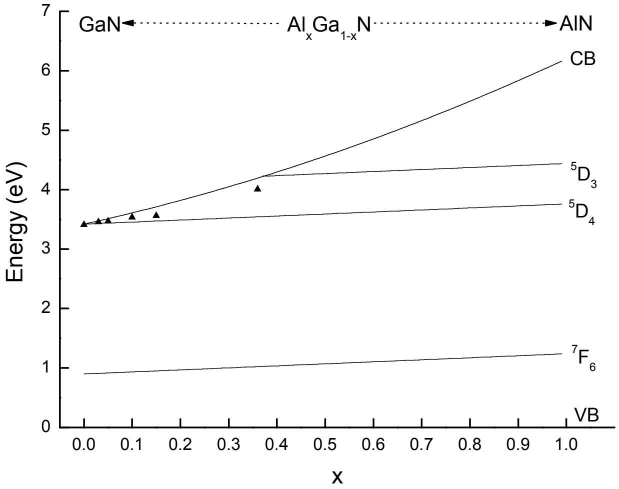

Fig. 5 The energy of the conducting band bottom (CB) and Tb energy levels relative to the valence band top (VB) as function of the Al content in $Al_xGa_{1-x}N$. The data points are the location of the $^5D_4$ state as derived from the energy barrier for thermal quenching.

Fig. 5 explains and predicts many features of Tb^{3+}emission in $Al_xGa_{1-x}N$. The $^5D_3$ state is located inside the conduction band below x=0.38 and emission from this state will not be possible at those compositions. Indeed studies up to x=0.15 did not reveal any $^5D_3$ emission at 8 K [11] whereas for x=0.54 $^5D_3$ emission is reported at 76 K [8,10]. Above x=0.38 the distance between the $^5D_3$ state and the conduction band increases with x. When thermal quenching proceeds via ionization of the $^5D_3$ electron to the conduction band, we predict that the emission from $^5D_3$ becomes more temperature stable with increasing x.

From the Arrhenius behavior of thermal quenching of emission intensity from the $^5D_4$ state but also from the shortening of emission decay time, the energy barrier for quenching is known at various compositions [8,10,11]. It increases from 0.008 eV for pure GaN to 0.15 eV for x=0.15, and the value for $T_{0.5}$ where the luminescence intensity drops by 50% increases from 27 K to 186 K. The data points in Fig. 5 are the location of the $^5D_4$ states below the conduction band as derived from these energy barrier values. Up to x=0.15 the predicted $^5D_4$ level location is consistent with the found barriers. However, an energy barrier of 0.19 eV reported by [10] for x=0.36 appears to disagree with expectation. Fig. 5 predicts that between x=0 and x=0.5, the quenching energy barrier for $^5D_4$ emission increases almost linearly with increasing x to a value of around 1 eV at x=0.5.

It is well established that the quenching of Eu^{3+} emission in phosphors for lighting or displays is via the charge transfer band of Eu^{3+}, and the quenching temperature increases with larger value for the charge transfer band. Tanaka *et al.* [28]

suggested this quenching mechanism in GaN. Since the energy of valence band electron to Eu^{3+} charge transfer increases from 3.15 eV in GaN to 3.5 eV in AlN, we expect that the energy barrier for quenching via the CT band should increase with about 0.35 eV. Data available are still limited. Wakahara *et al.* [8] reports a barrier of 0.17 eV for pure GaN and 0.23 eV for x=0.28 which confirms the trend predicted. Information for larger values of *x* was not found.

3.3 ZnO

ZnO is an emerging new compound and many studies are performed on its properties and its potential applications for future opto-electronic devices. The energy needed to create a free exciton in ZnO is 3.38 eV and excitation in this band leads to free exciton emission. We estimate the mobility bandgap energy for ZnO at around 3.4 eV. It is about the same as for GaN in Fig. 3. To locate the ground state levels of the divalent lanthanide impurities the energy of charge transfer to Eu^{3+} should be known. Several reports have appeared on the properties of Eu^{3+} doped ZnO, but a clear excitation band that can be identified as a charge transfer band was not reported. Yang *et al.* [32] did not observe a CT band in the excitation spectrum of red Eu^{3+} emission. Apparently the energy of CT to Eu^{3+} is higher or equal than the bandgap energy of ZnO. Jia *et al.* [33] prepared ZnO:Eu^{3+} codoped with F^- for charge compensation. They claim a much more efficient Eu^{3+} emission. The excitation spectrum reveals an excitation band starting just below the band edge. This can be the onset of the Eu^{3+} CT band. Possibly the presence of F^- charge compensator centers stabilizes the Eu^{3+} impurity leading to a lower energy CT band.

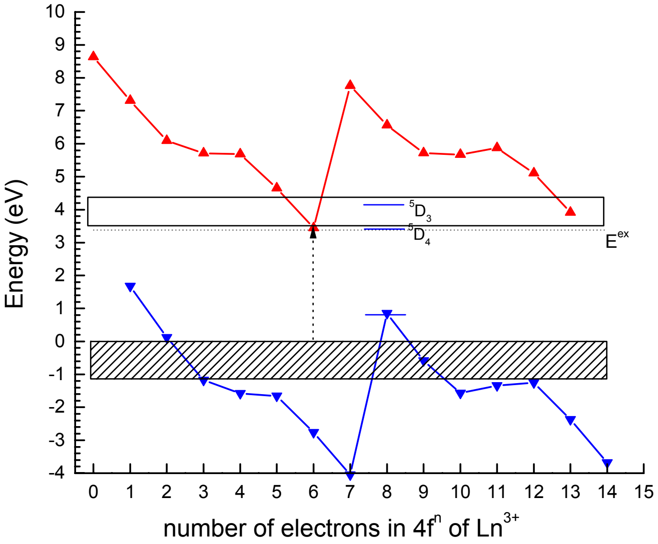

Fig. 6 The proposed location of the lowest 4f states of divalent and trivalent lanthanides in ZnO. The top of the valence band is at energy zero. The ZnO exciton state is at 3.38 eV. Optical transitions (arrows) and relevant excited and ground state 4f level locations (bars) are shown.

In the scheme of Fig. 6 we tentatively estimate the location of the Eu^{2+} ground state at or just below the bottom of the conduction band. Interestingly, ZnO:Eu^{3+} acts as a n-type semi-conductor with activation energy of 0.19 eV [32]. We may speculate that based on the energy level location of the Eu^{2+} ground state, Eu^{3+} acts as a shallow electron trap leading to the n-type semiconducting properties. To draw the ground state energies for the other divalent lanthanides curve d) from Fig. 2 was used. Note for GaN and AlN we used the other curve c). To draw the ground state energies for the trivalent lanthanides we will base on information on the Tb^{3+} emission. Pereira *et al.* [34] observed Tb^{3+} emission in nanocrystals of ZnO at 7 K that origins from the $^5D_4$ state. Emission from the $^5D_3$ state is not reported. In our view this means, like for GaN, that the $^5D_4$ state is located below and the $^5D_3$ state above the bottom of the nanocrystalline ZnO conduction band. Quantum size effects increases the energy of the delocalized conduction band state but not those of the localized Tb^{3+} 4f states [34]. Altogether we arrive tentatively at the scheme shown in Fig. 6. Both the ground state of Eu^{2+} is and the $^5D_4$ state of Tb^{3+} are near the edge of the conduction band. In this scheme the value of $\Delta E(Eu)$=6.2 eV which is nearly the same as for YPO_4 in Fig. 1. The scheme predicts that the emission from the $^5D_4$ state of Tb^{3+} is sensitive to temperature and quantum size effects.

4. SUMMARIZING REMARKS AND CONCLUSIONS

The change of level position of the lanthanide ions with changing type of lanthanide is well established by the universal double seated curves of Fig. 2. The precise positioning of these curves is however less well established and depends on the type of compound, the site occupied by the lanthanide ion, and possible effects of (charge compensation) defects or. The level positioning in GaN and AlN relies heavily on the energy of charge transfer to Eu^{3+} and on the energy barrier for quenching of the $^5D_4$ state of Tb^{3+}. Often these energies can be determined with reasonable accuracy but it is not fully established how accurate these energies represent the true location of the Eu^{2+} ground state above the valence band or the Tb^{3+} $^5D_4$ state below the conduction band. We estimate these systematic errors of the order of 0.3 eV.

We further assumed that curves a) and c) in Fig. 2 describe the change in level position with type of lanthanide ion. By determining the energy of charge transfer to Yb^{3+} in GaN and AlN the use of curves a) and c) in Fig. 3 and Fig. 4 can be justified or otherwise a slightly modified curve can be proposed. Also by determining the energy of the Eu^{3+} CT band as function of x, the linear interpolation used for Fig. 5 can be verified. Furthermore, the predictions on Tb^{3+} emission properties with changing x made in this work can be experimentally verified or falsified, and new data can be used to further refine the level scheme energies. Especially one may test at what value for x the $^5D_3$ emission starts to appear in $Al_xGa_{1-x}N$ alloys. For constructing the scheme of ZnO there is even no evidence for the CT band to Eu^{3+}, nevertheless we are the opinion that the proposed scheme can not be too far from the actual scheme, and possible errors tend to be very systematic. The value for $\Delta E(Eu)$ can be somewhat different leading to wider or smaller spacing between the divalent and trivalent states. The entire diagram can be shifted up and down a few 0.1 eV relative to the host bands. The entire diagram can also be tilted between the two configurations of Fig. 2. However, as it looks now the spacing, the shifting, and the tilting behaves in a gradual and systematic manner with changing type of compound. Therefore the margins of errors are relatively small.

When more accurate date become available or specific studies are performed the schemes can be further refined. Note that the absolute level location critically depends on the environment around the lanthanide ion. Therefore materials synthesis, presence of defects etc. may also affect the absolute location of level energies. Nevertheless schemes like in Fig. 1, 3, 4, and 6 form a good and necessary basis to start interpretation of spectroscopic and luminescence properties of lanthanide doped III-V and II-VI semiconductors.

An aspect not addressed in this work relates to charge carrier trapping and charge carrier donating properties of lanthanide doped compounds. Whenever an occupied lanthanide state is located above the top of the valence band, that state may act as a hole trap. This is the case for example for Ce^{3+}, Pr^{3+}, and Tb^{3+} in GaN and AlN. On the other hand when an unoccupied lanthanide level is located below the bottom of the conduction band that lanthanide may act as an electron trap. For example Eu^{2+} in GaN is located in Fig. 3 about 0.2-0.4 eV below the bottom of the conduction band. This implies that Eu^{3+} is an efficient electron trap and Eu^{2+} may act as electron donor.

REFERENCES

1. Hong Chen, Kuiyong Chen, D.A. Drabold, M.E. Kordesch, Appl. Phys. Lett. 77 (200) 1117.
2. M.R.H. Khan, Y. Koide, H. Itoh, N. Sawaki, I. Akasaki, Solid State Comm. 60 (1986) 509.
3. J. Sawahata, H. Bang, J. Seo, and K. Akimoto, Science and Techn. of Advanced Materials 6 (2005) 644.
4. K. Wang, R.W. Martin, K.P. O'Donnell, V. Katchkanov, E. Nogales, K. Lorenz, E. Alves, S. Ruffenach, and O. Briot, Appl. Phys. Lett. 87 (2005) 112107.
5. A.J. Steckl, M. Garter, D.S. Lee, J. Heikenfeld, and R. Birkhahn, Appl. Phys. Lett. 75 (1999) 2184.
6. E.E. Nyein, U. Hömmerich, J. Heikenfeld, D.S. Lee, A.J. Steckl, and J.M. Zavada, Appl. Phys. Lett. 82 (2003) 1655.
7. Chang-Won Lee, H.O. Everitt, D.S. Lee, A.J. Steckl, J.M. Zavada, J. Appl. Phys. 95 (2004) 7717.
8. A. Wakahara, Optical Materials 28 (2006) 731.
9. H.J. Lozykowski, Phys. Rev. B 48 (1993) 17758.

10. A. Wakahara, Y. Nakanishi, T. Fujiwara, A. Yoshida, T. Ohshima, T. Kamiya, phys. stat. sol (a) 202 (2005) 863.
11. Y. Nakanishi, A. Wakahara, H. Okada, A. Yoshida, T. Ohshima, H. Itoh, phys. stat. sol. (b) 240 (2003) 372.
12. P. Dorenbos, J. Phys.: Condens. Matter 15 (2003) 8417.
13. P. Dorenbos, J. Lumin. 111 (2005) 89.
14. C.W. Thiel, Y. Sun, R.L. Cone, J. of Modern Optics 49 (2002) 2399.
15. P. Dorenbos, E. van der Kolk, Applied Physics Letters 89 (2006) 061122.
16. P. Dorenbos, E. van der Kolk, Optical Materials in press (2007).
17. P. Dorenbos, J. Lumin. 91 (2000) 155.
18. P. Dorenbos, J. Lumin. 91 (2000) 91.
19. P. Dorenbos, J. Lumin. 104 (2003) 239.
20. L. van Pieterson, M.F. Reid, R.T. Wegh, S. Soverna, A. Meijerink, Phys. Rev. B65 (2002) 045113.
21. L. van Pieterson, M.F. Reid, G.W. Burdick, A. Meijerink, Phys. Rev. B65 (2002) 045114.
22. J. Andriesen, P. Dorenbos, C.W.E. van Eijk, Phys. Rev. B 72 (2005) 045129.
23. J.L. Pascual, J. Schamps, Z. Barandiaran, L. Seijo, Phys. Rev. B 72 (2006) 104105.
24. E. Nakazawa, J. Lumin. 100 (2002) 89.
25. A. Bessiere, P. Dorenbos, C.W.E. van Eijk, E. Yamagishi, C. Hidaka, and T. Takizawa, J. Electrochem. Soc. 151 (2004) H254.
26. P. Dorenbos, E.V.D. van Loef, A.P. Vink, E. van der Kolk, C.W.E. van Eijk, K.W. Krämer, H.U. Güdel, W.M. Higgins, and K. Shah, J. Lumin. 117 (2006) 147.
27. G. K. Liu, M. P. Jensen and P. M. Almond, J. of Phys. Chem. A 110 (2006) 2081.
28. M. Tanaka, S. Morishima, H. Bang, J.S. Ahn, T. Sekiguchi, K. Akimoto, phys. stat. sol. (c) 0 (2003) 2639.
29. H.J. Lozykowski, W.M. Jadwisienczak, A. Bensaoula, O. Monteiro, Microelectronics Journal 36 (2005) 453.
30. M.B. Kanoun, S. Goumri-Said, A.E. Merad, H. Mariette, J. Appl. Phys. 98 (2005) 063710.
31. Chang-Hong Kim, Il-Eok Kwon, Cheol-Hee Park, Young-Ju Hwang, Hyun-Sook Bae, Byung-Yong Yu, Chong-Hog Pyun, Guang-Yan Hong, J. Alloys and Compounds 311 (2000).
32. Chih-Cheng Yang, Suy-Yuh Cheng, Hsin-Yi Lee, San-Yuan Chen, Ceramics International 32 (2006) 37.
33. Weiyi Jia, Karem Monge, Felix Fernandez, Optical Mater. 23 (2003) 27.
34. A.S. Pereira, M. Peres, M.J. Soares, E. Alves, A. Neves, T. Monteiro, T. Trindade, Nanotechnology 17 (2006) 834.